Kinetics and Mechanism of the Simultaneous Carbothermic Reduction of FeO and MnO from High-Carbon Ferromanganese Slag

JAFAR SAFARIAN, LEIV KOLBEINSEN, MERETE TANGSTAD, and GABRIELLA TRANELL

The carbothermic reduction of 38.7 pct MnO-12.1 pct CaO-5.4 pct MgO-9.3 pct Al$_2$O$_3$-24.1 pct SiO$_2$-10.4 pct FeO slag in Ar at 1600 °C was studied using the sessile drop wettability technique. Pure graphite, coke, and charcoal were used as the carbon material substrates. The reduction rates were evaluated by sampling at different reduction times and by analyzing the chemical compositions of the reduced slag and the produced metal. The carbothermic FeO reduction from slag is initially fast followed by a much slower reduction rate. However, the rate of the MnO reduction is slow in the fast FeO reduction stage, and it starts to increase significantly during the slow FeO reduction stage. The kinetics of FeO and MnO reduction are affected by the type of carbonaceous materials. Moreover, the rate of the carbon dissolution/transfer into the produced metal phase and the amount of the transferred manganese to the metal phase depend on the type of carbon. Based on the experimental observations and the thermodynamic calculations, a mechanism for MnO reduction was proposed. According to this mechanism, MnO is mainly reduced through a metallothermic reduction by Fe and the rate of MnO reduction is controlled by the rate of the consumption of FeO from the slag, which takes place simultaneously. In contrast, the rate of FeO reduction in the fast initial reduction stage is controlled by the rate of the carbon dissolution/transfer into the metal phase. However, at the second slow FeO reduction stage, it is reduced mainly by the solid carbon.

I. INTRODUCTION

HIGH-CARBON ferromanganese (HCFeMn) is commonly produced in shaft electric furnace, which is also called a submerged arc furnace. In this process, manganese oxides in the burden are mostly reduced to MnO directly by CO gas. Subsequently, in the coke bed area of the furnace, where the process heat is generated, manganese is produced through the interaction of a high MnO-containing silicate slag with carbon:

$$MnO_{(l)} + C_{(s)} = Mn_{(l)} + CO_{(g)} \qquad [1]$$
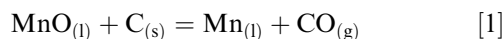
The carbothermic reduction of MnO from liquid slags and the effects of various parameters on its kinetics have been studied through several studies.[1–12] These studies have been mainly conducted in graphite crucibles with or without an initial metal phase. Stirring has no significant effect on the kinetics of MnO reduction, whereas the reduction rate is affected by the slag composition and temperature. Thus, it has been suggested that the reaction kinetics are not controlled by the diffusion of the

components in the bulk of the metal and slag phases and that they are controlled by the chemical reactions.[1–11] Also, the kinetics of MnO reduction is affected by the gas phase composition and different MnO reduction rates occur when different inert gases are used. Hence, it has been proposed that the carbothermic reduction of MnO is a mixed-control reaction that controls both the chemical reaction and the CO mass transfer in the gas phase.[12] The mechanism of MnO reduction from low and high MnO containing slags by the dissolved carbon in liquid iron is also well known.[3,5,6,10] According to this mechanism, MnO is reduced by Fe at the slag/metal interface and Mn and FeO are produced. Subsequently, FeO is reduced by CO gas at the slag/gas bubble interface, and Fe and CO$_2$ gas are produced; this reaction is followed by the regeneration of CO gas via the Boudouard reaction with the dissolved carbon in the metal at the metal/gas bubble interface.[3]

A few studies have been carried out to discover the effects of the carbonaceous material properties on the kinetics of MnO reduction. It has been observed that the reductant type influences the SiO$_2$ reduction from a MnO containing silicate slag significantly, although it does not have a large effect on the MnO reduction.[13,14] In contrast, it has been observed recently that the rate of MnO reduction from silicate slags is affected by the type of carbon material.[15,16] It has been observed that the existence of small Fe-Mn particles in the industrial ferromanganese slags increases the rate of the MnO

JAFAR SAFARIAN, Researcher, LEIV KOLBEINSEN, Professor, MERETE TANGSTAD, Professor, and GABRIELLA TRANELL, Professor, are with the Department of Materials Science and Engineering, Norwegian University of Science and Technology, Trondheim, Norway. Contact e-mail: Jafar.Safarian@material.ntnu.no.

reduction extensively.[16] Furthermore, a higher carbothermic FeO reduction rate from silicate slags that contain initial metal also has been observed.[17]

The objective of the current study is to investigate the MnO reduction from HCFeMn slag with different carbon materials and under the conditions of the existence of a metal phase in the system. In this case, the interaction of a synthetic slag that contains MnO and FeO with different carbon materials is studied using the sessile drop wettability technique. This helps us to simulate the situation of the real ferromanganese furnace, because usually some iron oxide is found in the furnace charge materials. It is also expected to have FeO reduction before MnO reduction. Therefore, MnO will be mainly reduced by carbon while a metal phase is present in the system.

II. METHODOLOGY

This study focuses on the interaction of a slag with carbon materials using the sessile drop wettability technique. The characterization and preparation of carbon substrates, the slag preparation, the sessile drop equipment, and the experimental conditions are described in the next subsections.

A. Carbon Materials

Three different carbonaceous materials consisting of pure graphite, a single coke produced from a single coal, and eucalyptus charcoal were used as the carbon material substrates. Powders of these materials were prepared and then pressed to make pellet disks with flat surfaces. To prepare the carbon powder substrates, they were crushed in a jaw crusher to less than 10 mm, ground in a tungsten carbide disc mill to a fine powder, and sieved to a size fraction of 44 to 105 μm. The charcoal powder was heat treated in CO gas at 1600 °C for 10 minutes to remove its large volatile materials content. These powders were then dried at 100 °C for 24 hours and were subsequently mixed with 3 wt pct stearic acid (binder) to achieve some green strength in the pressed substrates. The powder-binder mix was pressed into a small graphite crucible (10 mm outer diameter, 8 mm inner diameter, 3 mm height, and 1 mm deep) using 63.7 kg/cm^2 pressure.

A part of the study was dedicated to characterize the carbon materials. The proximate analysis of the carbon materials was determined. The specific surface area of the carbon powders was measured by Brunauer, Emmett, and Teller method using helium-nitrogen gas

as the surface adsorbate agent. The structural parameters such as carbon layer spacing (d_{002}) and the average crystallite size ($L_{C\ (002)}$) were determined using X-ray diffraction and applying the developed procedure by Iwashita et al.[18] Moreover, the CO_2 reactivity for carbonaceous materials was measured by thermogravimetery at 1000 °C in a 100 pct CO_2 atmosphere on the particles that ranged from 1.68 to 3.36 mm in size. The mass loss changes during the experiment were subsequently converted to the initial reaction fraction X of the sample mass. The changes in the initial reaction fraction with time (dX/dt), which were fairly linear, were calculated and used to characterize the CO_2 reactivity. The carbon material characterization has been described in detail,[19] and the results are summarized in Table I.

B. Synthetic Slag

High purity (+99.99 pct) fine powders of CaO, MgO, SiO$_2$, and Al$_2$O$_3$ were mixed in a ratio of CaO/MgO = 2, CaO/Al$_2$O$_3$ = 1.34, and Al$_2$O$_3$/SiO$_2$ = 0.4. The mixture was then melted in a graphite crucible in air and higher than 1600 °C using an induction furnace. The obtained slag was crushed in a tungsten carbide disc mill to a fine powder and was then mixed with appropriate amount of high purity MnO (+99.95 pct) fine powder by hand in plastic containers. The obtained mixture was melted in graphite crucible in air at 1550 °C. The produced slag was again crushed in the tungsten carbide disc mill to a fine powder and was then mixed with pure 99.5 pct FeO powder (CAS: 1345-25-1 from Alfa Aesar GmbH & Co KG, Karlsruhe, Germany). The mixture was melted in platinum crucible in air at 1550 °C. The slag composition was measured by electron probe microanalyzer (EPMA) and the composition in wt pct was 38.7 pct MnO-12.1 pct CaO-24.1 pct SiO$_2$-9.3 pct Al$_2$O$_3$-5.4 pct MgO-10.4 pct FeO. It is worth noting that a portion of Fe^{2+} and Mn^{2+} are oxidized to Fe^{3+} and Mn^{3+} during the melting in air. These oxides will be reduced rapidly again to Fe^{2+} and Mn^{2+} in the slag reduction experiments through reduction by carbon. In the present study the measured elemental Fe and Mn in the slags by EPMA were converted to their oxides in the form of FeO and MnO.

C. Experimental Details

The sessile drop wettability technique was used to study the interaction between the synthetic slag and the carbon substrates. A schematic diagram of the experimental set up is shown in Figure 1. The carbon substrate was located in the graphite sample holder, and a

Carbon Type	Fix C (wt pct)	Ash Content (wt pct)	Surface Area, SS (cm^2/g)	Sulphur Content (ppm)	d_{002} (Å)	Crystallite Size, L_C (Å)	Amorph. Fraction (pct)	CO$_2$ Reactivity (10^{-3}/min)
Graphite	99.9	0.04	32,000	—	3.364	553.35	—	1.17
Coke	89.39	10.11	11,100	4800	3.47	12.9	0.85	4.85
Charcoal	99.5	0.53	38,600	20	3.8	11.5	0.69	7.23

Table I. The Properties of the Carbonaceous Materials

40 ± 1-mg slag particle was put on the carbon surface. The furnace chamber was evacuated initially, and then the furnace was heated up slowly in pure argon (99.9999 pct Ar) with 0.5 Nl/min flow rate. The furnace was heated to 950 °C in approximately 10 minutes, followed by a rapid heating rate of 120 °C/min to 1400 °C, and held for 4 minutes at 1400 °C. The furnace was then heated up from 1400 °C to 1600 °C in 1 minute, and then it was held for reaction times of 2, 5, and 8 minutes with rapid cooling. The first 4-minute reduction at 1400 °C was required to maintain a relatively slow FeO reduction stage so that the pressed powder substrate was not destroyed. The temperature was controlled using a Keller PZ40 two-color pyrometer (Keller GMBH, Ibbenburen, Germany) focused on the edge of the graphite sample holder. A video camera (XCD-SX910CR; Sony, Tokyo, Japan) was used to record images from the sample at 960 × 1280 pixels.

The experiments were carried out through the stop of reduction within the above-mentioned reduction times to obtain the kinetic data points. After the experiments were completed, the samples were quenched, mounted in epoxy, and prepared for EPMA supported by wavelength dispersive spectroscopy (WDS). The slag and metal chemical compositions were measured in ten different points of each phase, and the averages were considered as the total slag and metal compositions. It is worth noting that the proper reproducibility of the experimental technique has been already observed by the authors for MnO reduction from a silicate slag by graphite substrates at different temperatures.[15,19]

III. RESULTS AND DISCUSSION

The thermodynamics of the slag reduction and the results of the reduction experiments are presented and discussed in this section. Moreover, based on the observed reduction kinetics and the chemical reactions in the system, the mechanism of slag reduction is explained.

A. Slag Reduction Thermodynamics

The ternary phase diagram for $(MnO + FeO)$-SiO_2-$(CaO + MgO + Al_2O_3)$ slag system ($MnO/FeO = 4$, $CaO/MgO = 2$, $CaO/Al_2O_3 = 1.34$) at different temperatures between 1180 °C and 1680 °C was calculated using FactSage thermodynamics software (FactSage 5.5; C.R.C.T.-Ecole Polytechnique de Montreal, Quebec, Canada) as illustrated in Figure 2(a). Assuming a negligible SiO_2 reduction, the $(MnO + FeO)$ content of slag during reduction changes along a straight line and forms a completely liquid slag above 1400 °C. The reduction of FeO mainly takes place before the MnO reduction because of the greater MnO stability. Thus, the slag chemical composition changes through the reduction from point A to point B with mostly FeO reduction. When the FeO content is relatively low, MnO is reduced from the MnO-SiO_2-$(CaO + MgO + Al_2O_3)$ slag system and from point B in Figure 2(b). The MnO reduction from this point takes place again from a completely liquid slag above 1400 °C. Regarding the reduction of FeO and MnO from a liquid phase, their activities are changed with the changes of FeO and MnO concentrations during reduction. These changes were also calculated by the FactSage (FACT oxide database) for 1600 °C as illustrated in Figure 3.

B. The Rates of FeO and MnO Reduction

Although the wettability technique was applied in the current study, the wettability parameters such as the contact angle, the rate of contact angle changes, and the contact area between the slag and carbon substrate were not used to discuss the reduction kinetics. Because considerable gas bubble formation and coexistence of the gas phase in the slag droplet make it difficult to measure the contact angle and the slag drop volume properly. Hence, the changes in the chemical compositions of the slag and the produced metal during reduction were considered to study the reduction kinetics.

The slag chemical analysis of the reduced slag indicated that the chemical composition around the slag phase is more less the same and that it is not dependent on the distance from the slag/metal and slag/carbon interfaces. It is worth noting that the standard deviation was small, which indicates that the EPMA is reliable. For example, the standard deviation for MnO concentration in 10 analyzed points was 0.4 wt pct, whereas the average MnO concentration was 38.7 wt pct. Figure 4 shows the changes in the FeO
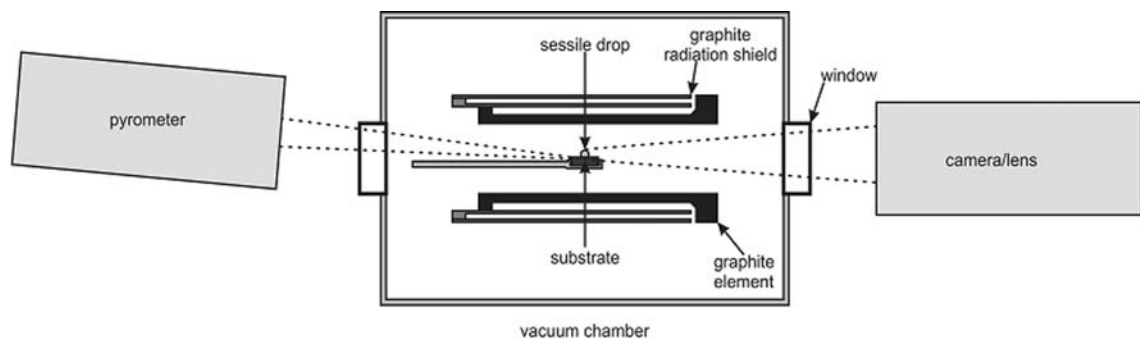

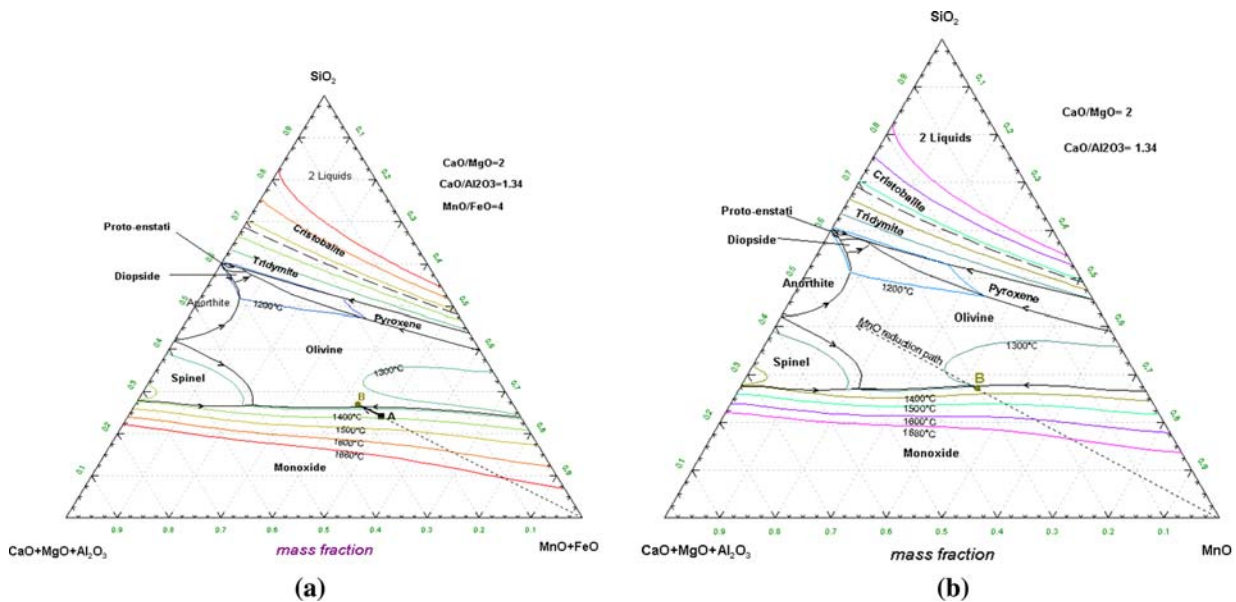Fig. 1—Schematic diagram of the experimental setup.

Fig. 2—(FeO + MnO)-SiO$_2$-(CaO + MgO + Al$_2$O$_3$) slag system and the FeO reduction path (a), and MnO-SiO$_2$-(CaO + MgO + Al$_2$O$_3$) slag system and the MnO reduction path (b).
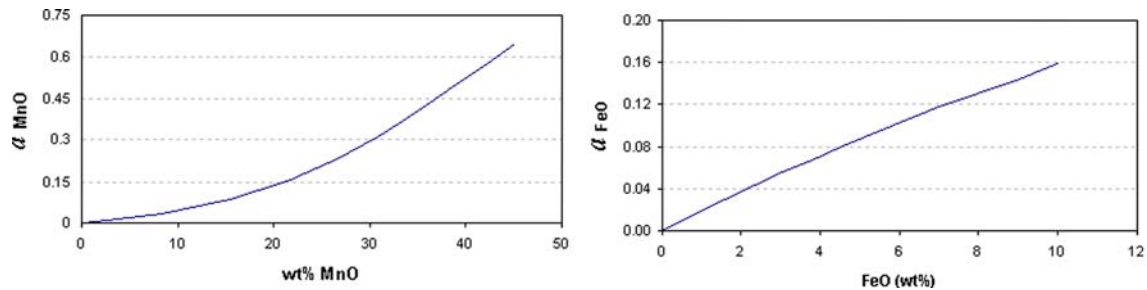

Fig. 3—The calculated changes in the FeO and MnO activities of slag during reduction at 1600 °C.

and MnO contents of slag through reduction with carbon reductants. Although the FeO activity in the slag is always less than the MnO activity (Figure 3), FeO reduction takes place with a much faster reduction rate because of the lesser thermodynamic stability than MnO. Figure 4 indicates also that the FeO reduction rate is dependent on the type of carbon material and that the greatest reduction rate is obtained with the coke and the least reduction rate is obtained with the graphite. The reduction of FeO takes place mainly at the first few minutes, and it is approximately completed for coke in 4 minutes, for charcoal in more than 4 minutes, and for graphite in around 7 minutes. Figure 4 shows that the MnO content of slag increases initially because of the FeO reduction, and then it starts to decrease so that a *hump* for MnO concentration appears. When the FeO initial fast reduction stage is completed, the MnO concentration is approximately on the top of this hump. Obviously, the hump position for the reduction with coke is before the first sampling, whereas for graphite it is before the second sampling, and charcoal it is before or after the first sampling. In this article, the rapid part of the FeO

reduction is called the *main FeO reduction stage*, and the MnO reduction after reaching the hump of MnO is called the *main MnO reduction stage*.

The reduction rate of MnO from a slag with a similar composition as the current synthetic slag and without FeO content by the same reductants was studied previously,[19] and based on their importance in the current discussions, the results are represented in Figure 5. Comparing Figures 4 and 5 reveals that the rate of MnO reduction from slag that contains FeO (from the hump point) by each carbon material is significantly higher than that from slag devoid of FeO. During the reduction of the latter slag, no metal phase was observed at the slag/carbon interface because of the rapid evaporation of the produced manganese.[15,19] When metal is not present, the charcoal has the greatest reactivity with the slag and graphite has the lowest reactivity (Figure 5). Whereas, when metal is present, coke is the most reactive carbon material (Figure 4). It may be concluded that the kinetics of MnO reduction is affected by the type of carbon material, and it can be extensively changed through a metal phase in the system.
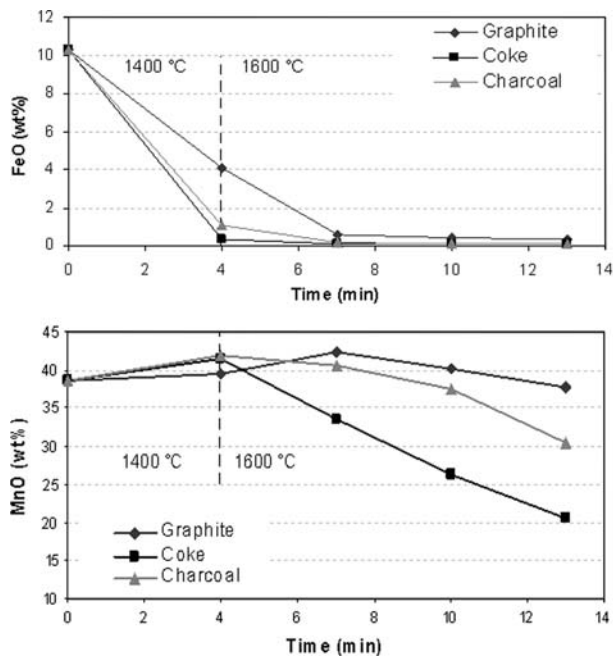
Fig. 4—The changes of the FeO and MnO concentrations in slag during reaction with carbon materials (pure liquid oxides were used as the standard state).
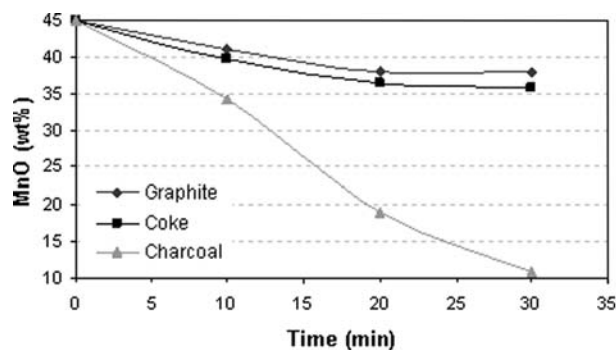

Fig. 5—The rate of MnO reduction from a slag similar to the synthetic slag of this study and devoid of FeO at 1600 °C in Ar.[19]

C. The Produced Metal

Microscopic studies of the cross sections of the samples revealed that a metal phase is always present at the slag/carbon interface, as typically shown in Figure 6. The measured concentrations of Fe, Mn, C, and Si in the metal produced by different carbon materials are listed in Table II and are shown in Figure 7 by solid lines. The initial Fe content was assumed 100 pct, because pure iron is expected to be first nucleated. As observed, the metal phase after a 4-minute reduction at 1400 °C includes a Fe-Mn-C alloy that contains a low Si content. The Mn/Fe ratio in the metal produced by coke is always the highest and by graphite is the lowest. The measured carbon concentrations in the produced metal phase are between 6.9 and 8.5 pct, except for the metals produced by graphite in 4 minutes and by coke in 13 minutes.
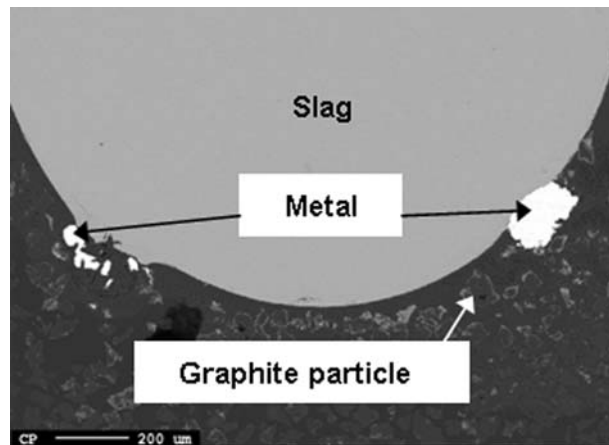

Fig. 6—The intersection of slag drop/graphite substrate after a 4-min reduction at 1400 °C.

Regarding the importance of carbon in the metal phase, the carbon solubility in metal produced by the carbonaceous materials was calculated by the formula suggested by Fenstad.[20] In this case, the measured Fe and Mn contents of the produced metal at various reduction times and the corresponding sample temperatures were considered. The calculated carbon solubilities in each alloy are listed and compared with the measured carbon concentrations in Table II. Moreover, these calculated carbon solubilities are illustrated on the carbon graph in Figure 7 by the dashed lines. Obviously, the measured carbon concentrations are higher than saturation, except for the metal produced by graphite in 4 minutes. This finding is expected with regard to the sample preparation for microprobe, where a thin layer of carbon was coated on the samples, which influences the resulting carbon concentrations higher than the actual carbon. It is worth noting that the reported measured carbon concentrations by EPMA in this article are around 10 random analyzed points of the metal drops, on average. For instance, the average carbon concentration in the metal produced through slag reduction by coke after 4 minutes is 6.7 wt pct with a standard deviation of 0.4 wt pct. The carbon graph in Figure 7 shows that the concentration of carbon is not significantly changed after exceeding around 6 wt pct, which indicates that the Fe-Mn alloys are approximately saturated above this level. Therefore, the metal is approximately carbon saturated in all coke and charcoal samples, except for the metal produced by graphite within a reduction time of 4 minutes. It is worth mentioning that the lower carbon concentration in the produced metal by graphite than by charcoal and coke in the first 4 minutes was confirmed by the microstructure studies. In particular, relatively lesser amounts of carbides were observed in the metal produced by graphite than that produced by charcoal, whereas they have similar concentrations of Mn. Although the measured carbon concentrations by WDS are not absolute and they always show higher concentrations than reality (because of the carbon coating), they can be used to indicate how much the metal produced by

Table II. The Measured Concentrations in the Produced Metal, and the Calculated Carbon Solubilities and Manganese Activities in the Metal Phase by the Proposed Formulas in Literature. Pure Liquid Fe and Mn Were Used as the Standard States for Activity Calculations

Carbon Substrate	Reduction Time (min)	Temperature (°C)	Measured Metal Concentrations (wt pct)				Calculated wt pct C_{sat}^*	Calculated $a_{Mn}^\dagger$
			Fe	Mn	Si	C		
Coke	4	1400	80.95	12.29	0.04	6.72	5.31	0.068
	7	1600	52.85	39.55	0.05	7.55	6.56	0.118
	10	1600	53.04	39.54	0.2	7.22	6.55	0.119
	13	1600	52.96	36.28	0.67	10.09	6.50	0.107
Charcoal	4	1400	91.25	1.76	0.01	6.98	5.04	0.013
	7	1600	67.94	25.31	0.03	6.72	6.16	0.094
	10	1600	62.08	29.83	0.01	8.08	6.29	0.101
	13	1600	46.54	44.82	0.09	8.55	6.72	0.126
Graphite	4	1400	94.89	0.44	0.02	4.65	5.00	0.003
	7	1600	81.32	11.01	0.01	7.66	5.79	0.055
	10	1600	81.97	11.01	0.02	8.0	5.79	0.055
	13	1600	80.54	11.01	0.21	8.24	5.79	0.055

*According to Fenstad[20]: log wt pct C $= 0.7005 + 1.12 \times 10^{-4}$ T $+ (-0.3550 + 0.99 \times 10^{-4}$ T)$R_{Fe} + (0.0294 - 0.082 \times 10^{-4}$ T)$R_{Fe}(1 - R_{Fe})$, $R_{Fe} =$ wt pct Fe/(wt pct Fe + wt pct Mn).
†According to Tangstad[8]: $a_{Mn} = X_{Mn} \cdot \exp (5.47X_c^2 - 46.8X_c^3 - 13.3X_cX_{Fe} + 17X_cX_{Fe}^2)$.
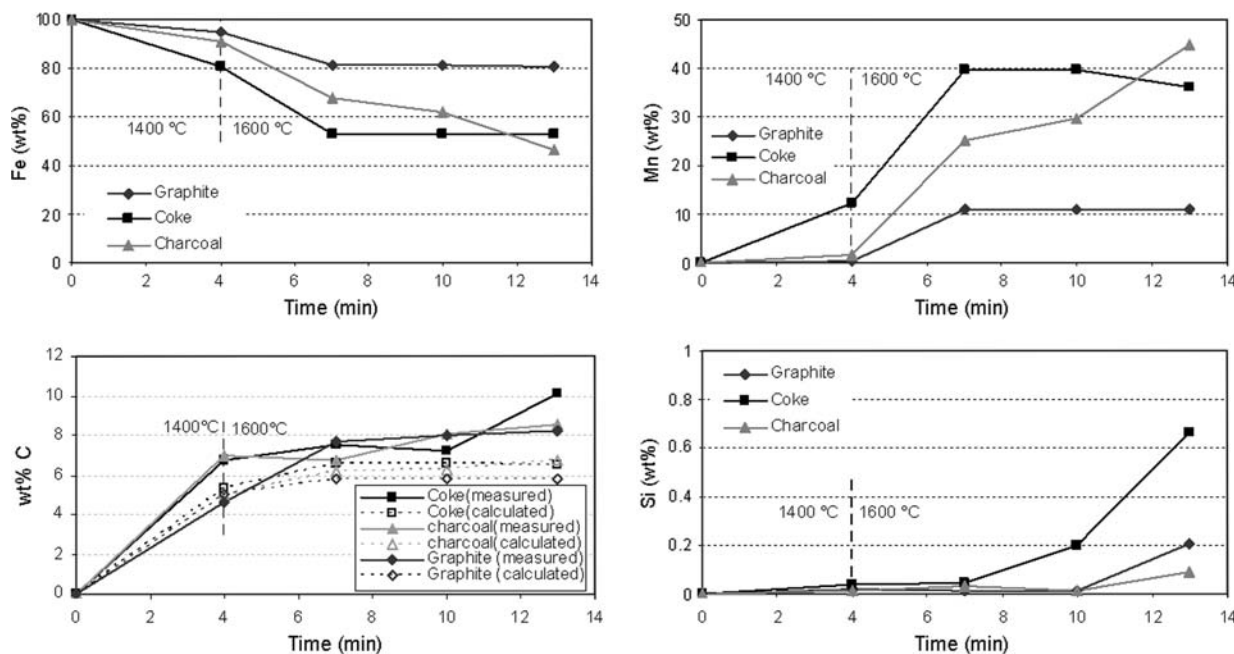

Fig. 7—The changes of the Fe, Mn, C, and Si concentrations in the metal phase during slag reduction by the carbonaceous materials.

graphite in 4 minutes is under saturation. Considering the reduction by coke as an outlier, the measured carbon concentrations in the metal phase are on average 1.2 ± 0.5 wt pct higher than the calculated concentrations for the carbon saturation in the alloys (Table II). This may indicate that the real carbon concentration in the metal produced by graphite within 4 minutes can be in the range 3.45 to 3.95 wt pct, which is less than the expected saturation of 5 wt pct (Table II).

The difference in the carbon content of the metals produced in the first sampling indicates that the rate of iron production with coke and charcoal is small

compared with the rate of carbon transfer/dissolution into the metal, so that the metal phase is always saturated by carbon. In contrast, the rate of metal production with graphite is relatively high compared with the rate of carbon dissolution/transfer in metal, and therefore, the carbon concentration of metal is below the saturation. Considering the carbon content differences and the rates of FeO reduction (Figure 4) with two carbon materials, we can say that the FeO reduction in the system is dependent on the carbon content of the metal phase, and FeO is mainly reduced by the dissolved carbon in the liquid metal. In this case,

Table III. The Initial Slag Mass and the Measured Slag Chemical Compositions of the Reduced Slags by Carbonaceous Materials

Carbon Substrate	Reduction Time (min)	Slag Initial Mass (mg)	Temperature (°C)	Measured Slag Concentrations (wt pct)					
				SiO$_2$	MgO	MnO	CaO	Al$_2$O$_3$	FeO
Coke	4	40.7	1400	26.49	5.98	41.37	13.72	12.08	0.36
	7	40.7	1600	30.81	7.06	33.54	15.86	12.61	0.104
	10	40.7	1600	33.99	8.14	26.37	17.56	13.86	0.073
	13	40.0	1600	35.89	9.06	20.55	18.85	15.59	0.062
Charcoal	4	40.9	1400	26.45	5.47	41.85	13.67	11.57	1.046
	7	40.1	1600	27.35	5.91	40.65	14.38	11.57	0.132
	10	39.6	1600	27.7	6.87	37.47	14.72	13.13	0.11
	13	40.9	1600	31.56	6.76	30.55	16.79	14.22	0.114
Graphite	4	41.2	1400	26.32	5.99	39.57	13.23	10.83	4.05
	7	40.8	1600	25.96	5.95	42.35	13.61	11.54	0.587
	10	41.0	1600	26.5	5.9	40.2	13.8	12.0	0.40
	13	41.0	1600	28.39	6.13	37.66	14.78	12.74	0.30

charcoal is a better source of carbon than graphite, because carbon dissolution/transfer in iron is not a rate-limiting step, although it can be rate limiting for the graphite.

D. Manganese Evaporation

The masses of the produced Fe and Mn through slag reduction were calculated using mass balance. In this case, the initial slag chemical composition, the initial slag mass, and the measured chemical compositions of the reduced slags (Table III) were used. Considering CaO and Al$_2$O$_3$ as the stable oxides in the slag phase, the mass of the reduced slags was calculated. The mass of the remained FeO and MnO was calculated with regard to the determined mass of the reduced slag and the measured slag composition. Consequently, the produced Fe and Mn for different reduction times were calculated. The obtained results (Figure 8) indicate that the Fe production is rapid at the beginning for all samples and that it levels off after 4 minutes at 1400 °C for coke and charcoal samples and later for the graphite sample (Figure 8(a)). In contrast, the manganese production starts slowly and simultaneously with the Fe production (solid curves in Figure 8(b)), and then it increases rapidly after the main FeO reduction stage. Figure 8(b) indicates that the amounts of the produced manganese after 4 minutes at 1400 °C for different reductants are close and in the range of 0.75 to 1.17 mg. However, the manganese concentration of the produced metal by different substrates is different, as illustrated in Figure 7. This indicates that the manganese evaporation occurs parallel to the manganese production (dotted curves in Figure 8(b)) and that it affects the total transferred manganese to the metal. Moreover, the Mn concentration in the metal levels off after awhile, whereas MnO is still reduced. This may indicate that the rate of Mn production and evaporation become similar after some reduction. Therefore, the manganese concentration in the metal does not vary, which is observed in particular for graphite and coke samples after 7 minutes in Figure 7.

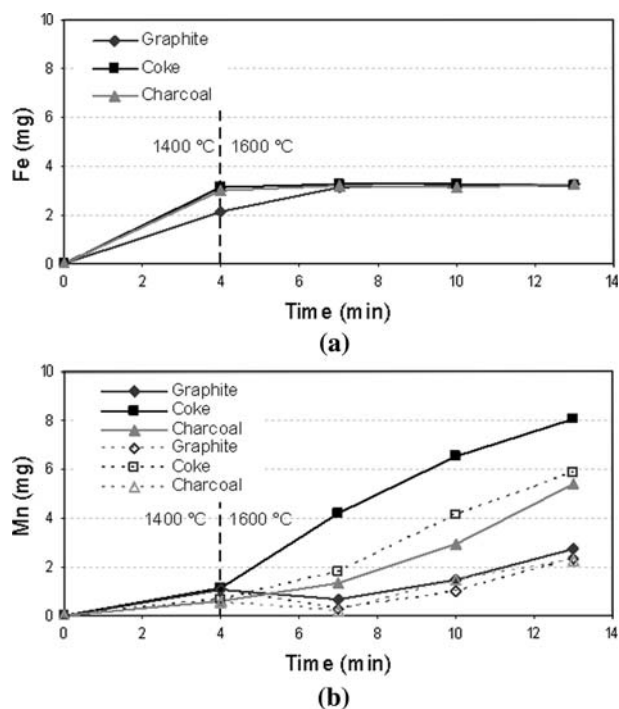Considering the Mn content of the metal phase in Figure 7 and the manganese production rate

Fig. 8—(a), The rate of Fe production, and (b), the rates of Mn production (solid lines) and Mn evaporation (dotted lines) through slag reduction by carbonaceous materials.

(Figure 8(b)), it is found that the concentration of Mn in the metal is mostly higher for the carbon samples with higher MnO reduction rates. The maximum Mn evaporation rate is about 0.5 mg/min for the coke sample. This evaporation rate is much lower than the Mn evaporation rate from the pure Mn at 1600 °C, which is about 5 mg/min as measured previously in Ar atmosphere by sessile drop method.[19] It is worth noting that when a similar FeO-free slag is reduced, no metallic Mn have been found at the slag/carbon interface, which indicates a faster Mn evaporation in Fe-free system.[19,21] This finding indicates that Fe plays an important role to stabilize the liquid state of the produced Mn with maintaining low Mn activity in the
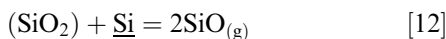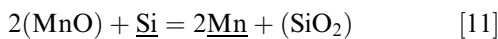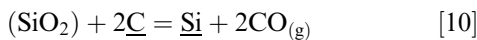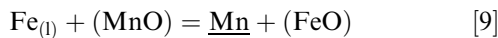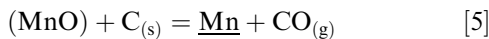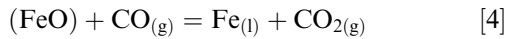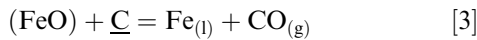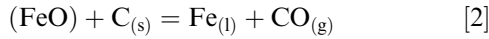
metal phase. This may show how Fe benefits the industrial process by decreasing the amount of Mn, which is evaporated in the coke bed area and condensed in the upper zones of the furnace.

E. The Chemistry of Slag Reduction

Regarding the above discussions, a possible explanation of the reduction mechanism pertaining to a slag containing MnO and FeO as well as SiO_2 is given in the next section in an effort to combine general knowledge about the possible reactions in the system and the experimental observations.

1. Chemical reactions

Overall, the following reactions may take place in the system:

$$(FeO) + C_{(s)} = Fe_{(l)} + CO_{(g)} \qquad [2]$$

$$(FeO) + \underline{C} = Fe_{(l)} + CO_{(g)} \qquad [3]$$

$$(FeO) + CO_{(g)} = Fe_{(l)} + CO_{2(g)} \qquad [4]$$

$$(MnO) + C_{(s)} = \underline{Mn} + CO_{(g)} \qquad [5]$$

$$(MnO) + \underline{C} = \underline{Mn} + CO_{(g)} \qquad [6]$$

$$(MnO) + CO_{(g)} = \underline{Mn} + CO_{2(g)} \qquad [7]$$

$$C + CO_{2(g)} = 2CO_{(g)} \qquad [8]$$

$$Fe_{(l)} + (MnO) = \underline{Mn} + (FeO) \qquad [9]$$

$$(SiO_2) + 2\underline{C} = \underline{Si} + 2CO_{(g)} \qquad [10]$$

$$2(MnO) + \underline{Si} = 2\underline{Mn} + (SiO_2) \qquad [11]$$

$$(SiO_2) + \underline{Si} = 2SiO_{(g)} \qquad [12]$$

$$\underline{Mn} = Mn_{(g)} \qquad [13]$$

$$C_{(s)} = \underline{C} \qquad [14]$$
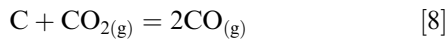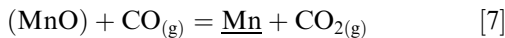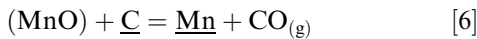
Obviously, some of the above reactions are combinations of the others. It is, however, helpful for the discussion of reaction mechanisms to consider these as well. Some of these reactions will, accordingly, be superfluous for equilibrium conditions. From a thermodynamics point of view, the Boudouard reaction [8] cannot proceed because of the use of pure argon flow over the sample and low oxygen partial pressure in the furnace chamber, which is $p_{O_2} = 1 \times 10^{-24}$ atm.[19] The details of the Boudouard reaction in an experimental set up similar to this study have already been studied by the

authors.[21] The slag reduction experiments are conducted under Ar gas flashing through the furnace chamber; thus, reactions [4] and [7] are probably not important. It is worth noting that if a CO-CO_2 gas film can exist locally at the slag/metal interface, then reactions [4] and [7] can take place with simultaneous reaction of the produced CO_2 with the dissolved carbon in the metal [reaction [8]]. This means that reaction [3] involves subreactions [4] and [8], and reaction [6] involves subreactions [7] and [8]. Regarding the point that the Boudouard reaction in the system is uncertain, the overall results of reactions [3] and [6] are considered in the discussions of this study.

Reaction [2] is dominating initially for FeO reduction, where Fe metal is first formed. From a thermodynamics point of view, reaction [2] is the first possible reaction in the system and it takes place at least for a small extent with an unknown mechanism. Because this reaction involves the coexistence of four phases and they can contact only at a point, it is probably limited to some active sites at the slag/solid carbon contact area. This reaction leads to the formation of new reaction areas in the system as slag/gas, metal/gas, slag/metal, and metal/carbon interfaces, and reaction [2] will consequently proceed through combination of subreactions [3], [4], and [8], as well as subreaction [14]. The kinetics and mechanism of FeO reduction by the dissolved carbon in liquid iron through these subreactions has been studied already.[3,5,6,10,17] According to Pomfret and Grieveson,[3] reaction [3] takes place through subreactions [4] and [8] at the slag/gas and at the gas/metal interfaces, where a gas layer exist at the slag/metal contact area. The dissolution/transfer rate of carbon to the metal can affect reaction [3] regarding the different carbon materials. For instance, reaction [3] might be slower for graphite substrate than for coke substrate because of the slower carbon transfer rate from graphite into the liquid iron, because the FeO reduction kinetics is dependent on the carbon concentration in the liquid Fe-Mn alloys.[10]

The reduction of MnO by carbon starts parallel with, and it continues along with, the FeO reduction. Because reactions [5] and [6] involve four and three phases, respectively, they are limited to reaction points and lines in the system. However, MnO reduction can potentially take place at the slag/metal contact area and between only two phases through reactions [9] and [11] as discussed below.

2. MnO reduction by Fe

The relationship between a_{FeO}/a_{MnO} and a_{Mn}/a_{Fe} at equilibrium for reaction [9] and different areas for the Gibbs free energy of this reaction are shown in Figure 9. Obviously, the reduction of MnO by Fe is always possible as long as the Mn content of the metal phase is low. Thus, MnO is reduced by the produced iron in the system from the beginning; however, the extent of the reaction is small, because Mn is transferred to a small amount of iron and the Mn content will increase rapidly toward an equilibrium or steady-state level. Moreover, large FeO reduction extents are required for small increase in the Mn content of the metal. This can be better understood with considering the equilibrium
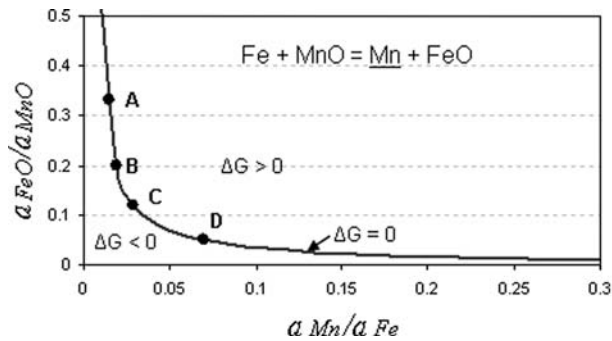
Fig. 9—The relationship between the changes in a_{FeO}/a_{MnO} and a_{Mn}/a_{Fe} at equilibrium for reaction [9] at 1600 °C.

Fig. 10—The intersection of the slag drop after a 7-min reduction at 1400 °C by graphite.

conditions at points A and B in Figure 9. As observed, increasing the Mn content of the melt from situation A to situation B requires a large decrease in the a_{FeO}/a_{MnO} ratio (a large FeO reduction extent). In contrast, at low a_{FeO}/a_{MnO} ratios, a little decrease in a_{FeO}/a_{MnO} will increase the a_{Mn}/a_{Fe} in a large extent, which means a large Mn transfer to the melt will occur. This can be resulted considering the changes from situation C to situation D in Figure 9. In short, MnO reduction by Fe is extensively possible, particularly at low FeO contents in the slag.

The metallothermic MnO reduction by Fe is also confirmed by examining Figure 4. For slag reduction by coke, the FeO content decreases faster than the other samples, and the MnO reduction at a high rate starts earlier than others. In contrast, FeO reduction by graphite substrate is slower and getting low FeO concentrations requires longer times, so the fast reduction by Fe is postponed. Considering Figures 4 and 9, and using the activity data in Figure 3, it is observed that reaction [9] proceeds considerably below about 1 pct FeO in the slag. This can prove why the starting point of rapid MnO reduction occurred before the first sampling for the coke, around the first sampling for the charcoal, and before the second sampling for the graphite. The slower MnO reduction rate by charcoal than by coke may indicate that the MnO reduction by Fe is linked to another reaction, such as reactions [2] and [3].

3. MnO reduction by Si

Reaction [11] is thermodynamically possible in the system and even for low SiO_2 activities. However, this reaction is dependent on the supply of Si through reaction [10], where Si is produced and transferred to the metal phase. The silicon reduction takes place at the slag/metal interface, because the formation of Si metal requires a low Si activity.[14] Thus, MnO reduction with silicon is controlled by reaction [10]. However, reaction [10] mostly takes place at the slag/metal/carbon line, where CO gas desorption, which is the rate limiting step of reaction [10], preferably takes place.[22] Thus, regarding the small slag/metal/carbon interfacial area, it is reasonable to assume that slow Si transfer to the melt occurs, so that the reduction of MnO by silicon is much less than the reduction by Fe. It is worth mentioning
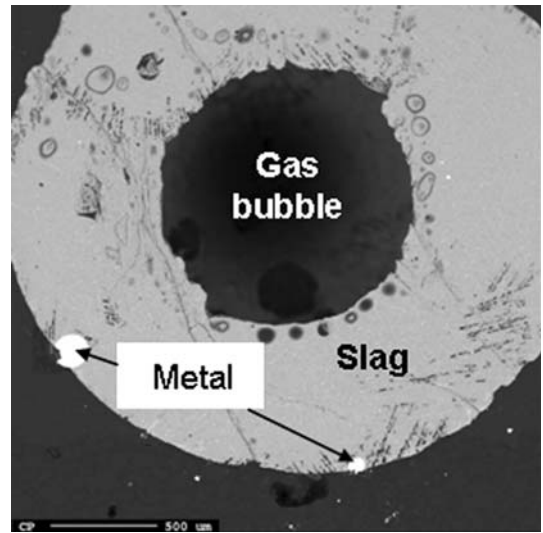
that at low MnO contents of the slag and high Si contents in the metal phase, the effect of the silicothermic reaction is not negligible.

F. The Gas Bubble Formation

It was observed in the sessile drop experiments that the slag droplet moves and dances during reduction. This phenomenon is caused by the CO gas bubble formation and growth in the slag and its bursting on the slag drop surface. The cross section of the reduced slag by the graphite substrate in Figure 10 shows that a gas bubble has been trapped during cooling, while it was passing through the slag. The formation and growth of the gas bubbles in the slag can indicate that the reduction reactions take place extensively by the dissolved carbon in the metal through reactions [3] and [6] at the slag/metal interface. If the reactions do not take place at this interface and they occur at slag/solid carbon interface, then no bubbling is expected, because in such situations, the released gas through the chemical reactions would prefer to leave the interface through the powder substrate and does not penetrate to the slag. It is worth noting that many small metal prills, even of submicron size, were observed in the solidified slag drop, and they may react with the slag as well. These metal prills have been transferred into the slag through the gas bubbles and the fluid flow in the slag droplet. Regarding the small size of these metal prills, it may be reasonable to assume it is a suspended metal phase in the slag. The role of iron in the mechanism of MnO reduction may also be confirmed with regard to the composition of the metal prills, which are distributed in the whole slag. It was observed that these metal prills are Fe-Mn-C alloys with much less carbon than the large metal particles at the slag/carbon interface. This finding may show that the transferred metal prills to the slag react with slag and decarburized.
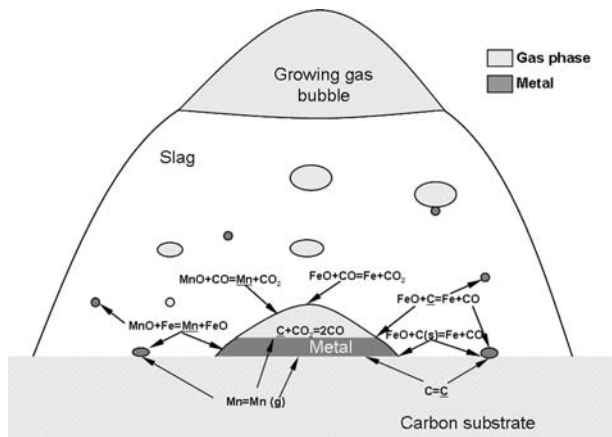
Fig. 11—A schematic of the slag reduction with regard to the possible involved reactions.

G. Summary of the Possible Mechanism of Slag Reduction

Considering the obtained results and the discussions, the carbothermic reduction of MnO from FeO-containing slags can be explained. To simplify the system, the drawn schematic for the important reactions and the slag-reduction mechanism in Figure 11 can be considered. As mentioned previously, the reduction of FeO in the main FeO reduction stage can occur by both the solid and dissolved carbon in the produced metal. Regarding the correlation between the FeO reduction kinetics and the dissolved carbon concentration in the melt (Figures 4 and 7), and also the extensive gas bubble release from the slag surface, it may be reasonable to consider the reduction of FeO by the dissolved carbon as the dominant reaction. And as discussed previously, the kinetics of this reaction are controlled by the solid carbon transfer into the produced metal. In this stage, the reduction of MnO by Fe takes also place because of the rapid formation of iron containing high activity. In this stage, the rate of MnO reduction is dependent on the rate of the FeO consumption in the system. This means that the reduction of both FeO and MnO in the main FeO reduction stage is controlled by the carbon dissolution/transfer into the produced metal phase.

Two possible mechanisms can be studied for the MnO reduction in the main MnO reduction stage. The first mechanism is the MnO reduction by the solid carbon according to reaction [5] and without Fe contribution. If such a reaction takes place in the system, then the order of sequence of the MnO reduction rates by carbonaceous materials in Figure 4 has to be similar to the MnO reduction rates from FeO-free slag (Figure 5). But, as we can observe, the order of the MnO reduction rates from theses two type of slags is different. Moreover, reaction [5] leads to the formation of CO gas at the slag/carbon interface with no bubble bursting from the slag. However, gas bubble bursting is always observed from the slag drop top, which means that reaction [5] cannot be dominant in the system. As described in section E, this reaction involves four phases, and it is limited to a few points in the system. In contrast, if this reaction proceeds at slag/carbon contact area without Fe contribution, it leads to the formation of a metal rich of Mn with high manganese activity. However, some metal in the system that contains Mn with low activity (Table II) already exists, which maintains better thermodynamic conditions for the reaction. Thus, MnO reduction does not take place in the system at the slag/carbon interface without the contribution of the metal droplets that contain iron.

A possible mechanism for manganese oxide reduction in the main MnO reduction stage can be MnO reduction by Fe through reaction [9] and then the reduction of the produced FeO by the solid carbon. This can be confirmed with obtaining similar MnO and FeO reduction rate orders with regard to the carbonaceous materials in both reduction stages (Figure 4). It was also observed that in the main MnO reduction stage, the metal phase is almost saturated of carbon. Therefore, if the FeO reduction by the dissolved carbon in the metal is dominant, then the corresponding MnO reduction rates for different substrates must not be significantly different, which is not observed in the experimental results (Figure 4). Hence, the FeO reduction in the main MnO reduction stage may occur mainly by the solid carbon through reaction [2]. This reaction involves four phases (slag, metal, carbon, and gas), and it seems to be impossible in the system. However, this reaction is the first reaction in the system after interacting the slag with carbon, and it may be reasonable to consider it as a proceeding reaction with an unknown mechanism in the main MnO reduction stage. This result can indicate that the kinetics of FeO reduction, and consequently the MnO reduction, in the second stage are dependent on the reactivity of the solid carbon material. Subsequent work would be beneficial to increase our knowledge about the mechanism details and to clarify the remaining uncertainties.

IV. CONCLUSIONS

The reduction of a silicate slag containing FeO and MnO by graphite, coke, and charcoal was investigated, and the following main points were obtained:

1. The carbothermic reduction of FeO and MnO from the slag takes place simultaneously. However, the initial rate of the FeO reduction is fast, and it is then followed by a slow reduction rate. But the MnO reduction is slow in the rapid FeO reduction stage and then the speed increases significantly.
2. The kinetics of FeO and MnO reduction is affected by the type of carbon. Slag is reduced by coke faster than by charcoal and much faster than by graphite.
3. When FeO is present in the slag, a metal phase at slag/carbon interface is maintained and it increases the rate of MnO reduction through reduction by Fe and the dissolved carbon.
4. The carbon dissolution/transfer to the metal phase can be the rate-limiting step for the FeO and MnO reduction in the rapid FeO reduction stage.
5. The MnO reduction in the main MnO reduction stage is dependent on the rate of simultaneous FeO

reduction, which is dependent on the reactivity of solid carbon material.

ACKNOWLEDGMENTS

OPEN ACCESS

REFERENCES

1. S.K. Tarby and W.O. Philbrook: *Trans. TMS-AIME*, 1967, vol. 239, pp. 1005–17.
2. W.L. Daines and R.D. Pehlke: *Metall. Trans.*, 1971, vol. 2, pp. 1203–11.
3. R.J. Pomfret and P. Grieveson: *Ironmaking Steelmaking*, 1978, vol. 5, pp. 191–97.
4. T. Shimoo, S. Ando, and H. Kimura: *J. Jpn. Inst. Met.*, 1984, vol. 48, pp. 922–29.
5. K. Upadhya: *ISS Trans.*, 1986, vol. 7, pp. 1–6.
6. K. Xu, G. Jiang, W. Ding, L. Gu, S. Guo, and B. Zhao: *ISIJ Int.*, 1993, vol. 33 (1), pp. 104–08.
7. T.A. Skjervheim: Ph.D. Dissertation, Norwegian Institute of Technology, Trondheim, Norway, 1994.
8. M. Tangstad: Ph.D. Dissertation, Norwegian Institute of Technology, Trondheim, Norway, 1996.
9. V. Olsø, M. Tangstad, and S.E. Olsen: *Proc. INFACON 8*, Chinese Society for Metals, Beijing, China, 1998, pp. 279–83.
10. S.Q. Guo, G.C. Jiang, J.L. Xu, and K.D. Xu: *J. Iron Steel Res. Int.*, 2000, vol. 7 (1), pp. 1–5.
11. B.A. Kukhtin, V.N. Boronenkov, O.A. Esin, and G.A. Toporishchev: *Russ. Metall.*, 1969, vol. 1, pp. 43–47.
12. M. Yastreboff, O. Ostrovski, and S. Ganguly: *ISIJ Int.*, 2003, vol. 43 (2), pp. 161–65.
13. K. Berg and S.E. Olsen: *SINTEF Internal Report*, SINTEF, Trondheim, Norway, 2004.
14. S. Gaal, K. Berg, G. Tranell, S.E. Olsen, and M. Tangstad: *7th Int. Conf. on Molten Slags, Fluxes and Salts*, Cape Town, South Africa, 2004, pp. 651–57.
15. J. Safarian and L. Kolbeinsen: *ISIJ Int.*, 2008, vol. 48 (4), pp. 395–404.
16. G. Tranell, S. Gaal, D. Lu, M. Tangstad, and J. Safarian: *INFACON XI*, New Delhi, India, 2007, pp. 231–40.
17. S.L. Teasdale and P.C. Hayes: *ISIJ Int.*, 2005, vol. 45 (5), pp. 642–50.
18. N. Iwashita, C.R. Park, H. Fujimoto, M. Shiraishi, and M. Inagaki: *CARBON*, 2004, vol. 42, pp. 701–14.
19. J. Safarian: Ph.D. Dissertation, Norwegian University of Science and Technology, Trondheim, Norway, 2007.
20. J. Fenstad: Ph.D. Dissertation, Norwegian University of Science and Technology, Trondheim, Norway, 2000.
21. J. Safarian, G. Tranell, L. Kolbeinsen, M. Tangstad, S. Gaal, and J. Kaczorowski: *Metall. Mater. Trans. B*, 2008, vol. 39B, pp. 702–12.
22. R.J. Pomfret and P. Grieveson: *Can. Metall. Q.*, 1983, vol. 22 (3), pp. 287–99.